

Article

Interaction among Controlling Factors on Riverine DIN Export in Small Mountainous Rivers of Taiwan: Inseparable Human-Landscape System

Wen-Shiuan Lee ¹, Jr-Chuan Huang ^{1,*} , Chung-Te Chang ^{2,*}, Shih-Chien Chan ³, Ying-San Liou ⁴, Chien-Sen Liao ⁵ , Li-Chin Lee ¹, Jun-Yi Lee ¹ , Yu-Ting Shih ¹ , Meng-Chang Lu ¹  and Pei-Hao Chen ¹

¹ Department of Geography, National Taiwan University, Taipei 10617, Taiwan; b06208033@ntu.edu.tw (W.-S.L.); d04228001@ntu.edu.tw (L.-C.L.); d02228001@ntu.edu.tw (J.-Y.L.); d00228003@ntu.edu.tw (Y.-T.S.); b99208035@ntu.edu.tw (M.-C.L.); d06228001@ntu.edu.tw (P.-H.C.)

² Center for Ecology and Environment, Tunghai University, Taichung 40799, Taiwan

³ Department of Geography, National Changhua University of Education, Changhua 50074, Taiwan; scchan@cc.ncue.edu.tw

⁴ Department of Natural Resources and Environmental Studies, National Dong-Hwa University, Hualien 974301, Taiwan; yingsan@gms.ndhu.edu.tw

⁵ Department of Civil and Ecological Engineering, I-Shou University, Kaohsiung 84001, Taiwan; csliao@isu.edu.tw

* Correspondence: riverhuang@ntu.edu.tw (J.-C.H.); chungtechang@thu.edu.tw (C.-T.C.)

Received: 21 September 2020; Accepted: 21 October 2020; Published: 23 October 2020



Abstract: Increasing anthropogenic nitrogen (N) emission via different pathways has shown prominent impact on aquatic ecosystems for decades, but the effects of interaction among climate-, landscape- and human-associated variables on riverine DIN (dissolved inorganic nitrogen, mainly NO_3^- and NH_4^+) export are unclear. In this study, the data of 43 watersheds with a wide range of climate-, landscape- and human-associated gradients across Taiwan were evaluated with partial redundancy analysis (pRDA) to examine their interactive controls on riverine DIN export. Results show that the annual riverine DIN export in Taiwan is approximately $3100 \text{ kg-N km}^{-2} \text{ yr}^{-1}$, spanning from $230 \text{ kg-N km}^{-2} \text{ yr}^{-1}$ in less disturbed watersheds (eastern and central Taiwan) to $10,000 \text{ kg-N km}^{-2} \text{ yr}^{-1}$ in watersheds with intensive human intervention (southwestern and northern Taiwan). NO_3^- is generally the single dominant form of DIN, while NH_4^+ renders significance in disturbed watersheds. Nearly all environmental variables display a positive correlation with DIN export, except for landscape setting variables (e.g., slope, area, channel length), which show a negative relationship. In terms of seasonal pattern, climate and human-landscape variables are related to NO_3^- export independently in the wet season, yet in the dry season climate-human variables jointly dominate NO_3^- export. Meanwhile, human-landscape (LH) variables (λ_1 of LH > 0.60) control NH_4^+ exports in both seasons, and human-associated (H) variables (λ_1 of H = 0.13) have a minor effect on NH_4^+ exports in dry season. Precisely, the contribution of controlling variables on DIN export vary with species and seasons, indicating water quality management could be time-dependent, which should be taken into consideration for designing mitigation strategies.

Keywords: dissolved inorganic nitrogen (DIN); redundancy analysis (RDA); partial redundancy analysis (pRDA); small mountainous rivers (SMRs); Taiwan

1. Introduction

Reactive nitrogen, a vital and essential nutrient for organisms and ecosystems, plays a key role in maintaining biodiversity and functions of ecosystems [1,2]. Over the past half century, the rapid increasing anthropogenic N emissions inevitably accelerated N deposition into the biosphere [3], and consequently exceeded the N-requirement for terrestrial ecosystems [4]. Studies show that N emissions and depositions have been declining in Europe and the U.S. since 2000, East and South Asia, in contrast, have become the hot spots of pollutant emissions due to population growth and intense agricultural activities [5,6]. Regions located near the emission source of East Asia receive excessive N deposition under favorable climatic conditions, such as the East Asian monsoon that blows directly to Taiwan with abundant rainfall [7]. The overloaded dissolved inorganic nitrogen (DIN) (majorly NO_3^- , and NH_4^+) led to eutrophication and harmful algal blooms which deteriorated water quality and caused damages in aquatic communities [8]. However, the DIN exports, particularly for seasonal changes, in subtropical mountainous watersheds are still unclear.

Many studies have demonstrated that even a mild replacement of natural vegetation with agricultural land use within watersheds would have significant impacts on hydrochemical processes [9, 10], especially for DIN export from non-point pollution sources [11–13]. Landscape features such as slope, soil type/moisture, channel length, watershed area and relief may also regulate water quality [14]. In addition, climatic factors play a principal role in nutrient cycling in the era of warming climate and increasing extreme events. A warmer temperature will accelerate biogeochemical processes that would alter enzyme reactions, e.g., nitrification and denitrification, via microbial activities [15]. The torrential rainfall caused by synoptic weather, such as thunderstorms and tropical cyclones during summer, can bring approximately 30% to 50% of annual precipitation, such that a considerable amount of DIN will be flushed out, as evidenced in Taiwan [11,12]. However, the effects of the independent and interactive relationship among landscape patterns, climatic factors and anthropogenic disturbance are still not clear on riverine DIN export [16].

Previous analyses widely used linear or non-linear regression models to estimate the DIN export, but failed to separate the collinearity among variables, which might violate the statistical independent assumption [17]. To tackle the issues of collinearity, a series of well-developed methods, namely, principal components analysis (PCA), redundancy analysis (RDA) and partial RDA (pRDA), have been utilized to clarify the relative importance of independent variables and their interactive effects on dependent variables [18,19]. In this study, we apply PCA and pRDA to evaluate the contribution of climatic-, landscape- and human-associated variables and their interactions on DIN export based on 43 island-wide watersheds in Taiwan. This synthesis can help to disentangle the intertwined effects of these fundamental environmental factors on the behaviors of nutrient fluxes. Specifically, the objectives of this study are to (1) quantify riverine DIN export in subtropical watersheds in Taiwan, (2) explore the interplay of human disturbance, climatic factors and landscape characteristics on riverine NO_3^- and NH_4^+ exports, respectively, and (3) figure out the spatial and seasonal variation of the controlling factors' influences on DIN exports.

2. Materials and Methods

2.1. Study Site

Taiwan, located in the northwest Pacific Ocean, is a tropical/subtropical mountainous island in the East Asian monsoon climate zone. Elevation ranges from sea level to approximately 4000 m in a short horizontal distance (<75 km). The Tropic of Cancer crosses the central part of Taiwan, which divides the island into tropical monsoon climate in the south and subtropical monsoon climate in the north. The mean annual temperature (MAT) is 22 °C across the island, ranging from 15.0 °C/18.2 °C in the north/south in January to 28.7 °C/28.4 °C in July, and the MAT decreases with increasing altitude [20]. The mean annual precipitation (MAP) is 2500 mm for the entire island but shows high spatial variability ranging from less than 1500 mm in southwest Taiwan to over 4000 mm in the mountains of northeastern

Taiwan [20]. There are more than 75% of MAP falls in the humid summer (May to October), while winter-spring (November to April) is a relatively dry period.

Natural forests, plantation and bamboo forests cover 60% of the land, while farmlands and urbanized areas occupy 29% and 11%, respectively (Figure 1). The dominant vegetation types and land cover of Taiwan change from mixed and conifer forests at the mid and high elevation (>2000 m a.s.l.), evergreen broadleaf forests at the low and mid elevation (200–2000 m a.s.l.) to urban, buildup area and farmland on coastal plains (<800 m a.s.l.) (Figure 1). In this study, in order to estimate island-wide watershed DIN export, our sampling scheme covers a total of 43 sites. Individual watershed represented by each site can be as small as 82 km² and as large as 2969 km², and as a whole, they occupy more than 70% of the island and distribute evenly across Taiwan (Figure 1). Twenty-nine of the 43 watersheds are majorly covered by natural forest (>70% of forest cover), while 14 of the 43 are situated in the transition between mountain and plain regions where agricultural land cover and buildup area account for 10–65% and 0–18%, respectively (Figure 1 and Table S1). The average slope of the watersheds varies from 8% to 76%.

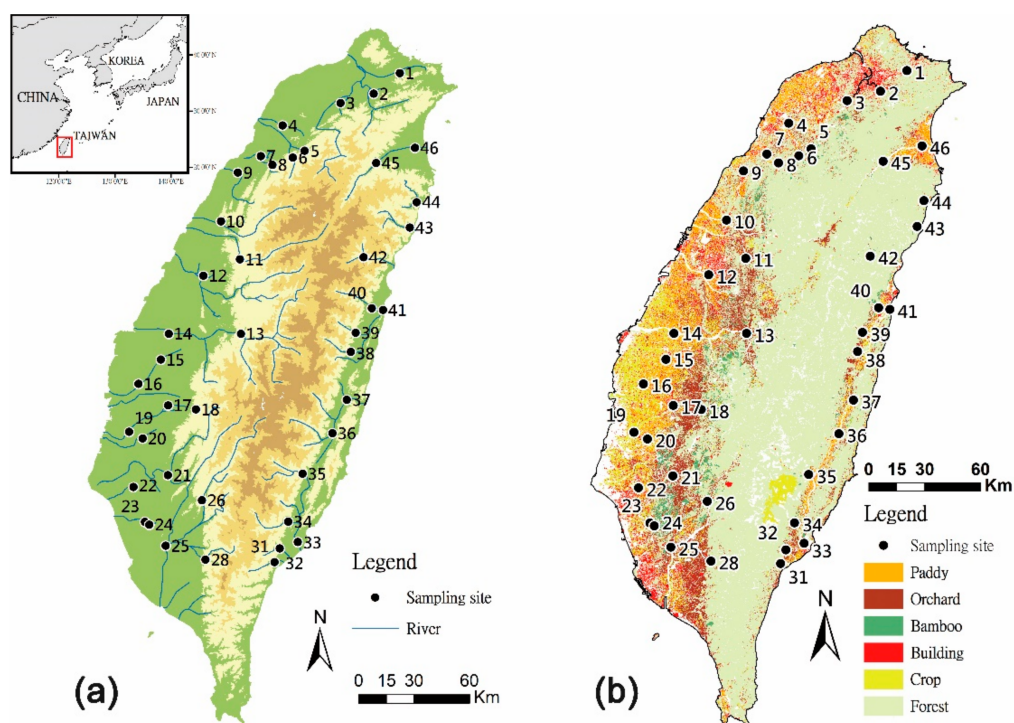


Figure 1. The geographical location of 43 sampling sites (a) and land cover map of Taiwan (b).

2.2. DIN Sampling and Streamflow Simulation

A monthly sampling scheme was conducted at all sampling sites (watersheds) during 2015–2016. Each route would be finished within 2 days. Stream water samples were collected by plunging a 1-L PE (polyethylene) bucket into stream, and the water was immediately filtered through 0.7 μm filters. A 15 mL subsample of filtrate was frozen on-site in liquid nitrogen and kept frozen until laboratory analysis at National Taiwan University. Nitrate, nitrite and ammonium content were analyzed using ion chromatography (IC) using a Dionex ICS–1500 (Thermo Fisher Scientific Inc.[®] Sunnyvale, CA, USA) with a detection limit of 0.2, 0.2, and 0.4 μM , respectively. Our DIN calculation includes NO_2^- , NO_3^- and NH_4^+ . Among them, nitrite is easily oxidized to nitrate and accounts for a small fraction (<5.0%). Therefore, we mainly analyzed and discussed NO_3^- and NH_4^+ .

Streamflow was acquired from the water level stations maintained by the Water Resource Agency (www.wra.gov.tw). The water level records were converted to streamflow via an individual rating curve

and cross section approach. For some periods of missing records and ungauged sites, a hydrologic model (HBV, the Hydrologiska Byråns Vattenbalansavdelning model [21]) was used to fill the data gaps [22]. The historical observed daily streamflow was utilized to train the parameter set to fit low, normal and extreme values of simulated streamflow using the performance measure of NSE (Nash-Sutcliffe efficiency coefficient) [23]. The calibrated parameter set was then applied to the watersheds using their own climatic inputs and terrain information to simulate their daily streamflow during 2015–2016.

2.3. Export Estimation

Based on the discrete NO_3^- and NH_4^+ concentration and continuous streamflow rates, individual NO_3^- and NH_4^+ export of the 43 sites were then estimated using an R software package, loadflex, which provides several common methods (e.g., interpolations, regressions and composite method) for export estimation [24]. The composite method synthesizing rectangular interpolation and regression models is applied for export estimation. The mean values of two export methods in 2015 and 2016 were used as export results for further analysis. The rectangular interpolation has usually been used for studies on solute and sediment exports, where horizontal lines are drawn through observations in a plot of concentrations against time, and each horizontal line is connected to the next by a vertical line midway between successive observations [25]. The regression approach is a longstanding interpolation in estimating watershed solute exports (Figure 2). It often requires less data than other models if the data can span over the range of predictors instead of the full time period of interest [26]. A simple regression equation based on observed nutrient concentrations and concurrent streamflow (Q) with an exponent function is used to represent the hydrological influence on transport as Equation (1) below:

$$\text{EXPORT} = m \sum_{j=1}^T Q_j C_j = m \sum_{j=1}^T Q_j e^{a_0 + a_1 \ln Q}, \quad (1)$$

where Q_j [mm d^{-1}] is the daily streamflow rate on j -th day; C_j [mg-N L^{-1}] is an estimated concentration of NO_3^- and NH_4^+ on the j -th day, m is the conversion factor to convert the calculated values into a specific unit [$\text{kg-N km}^{-2} \text{ yr}^{-1}$], and a_0 and a_1 are regressive coefficients. Coefficient a_0 is generally highly associated with the mean of observed nutrient concentration, and a_1 indicates the hydrological influence. A larger coefficient, a_1 (>0), indicates enhanced concentration with increasing streamflow, whereas a smaller value reflects the dilution effect because concentration decreases with the increase of discharge percentage. From Equation (1), we can estimate the concentration and export for non-measured days by introducing continuous daily streamflow [27]. According to the hydrologic seasonality, we summarized the daily export from May to October as wet season export and the summation of other daily exports as dry season export.

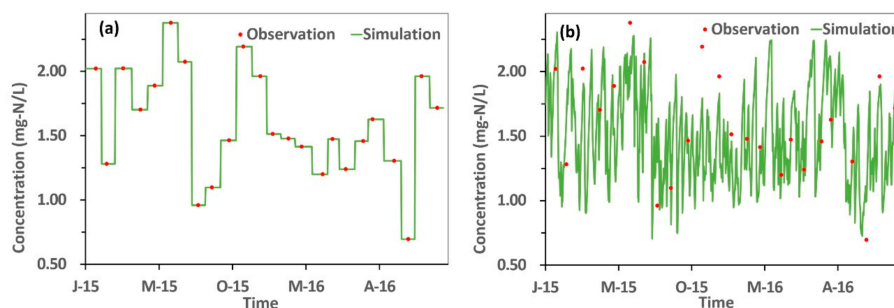


Figure 2. The model-fitted NO_3^- concentration of site no.1 for an unmeasured time sequence based on (a) a rectangular interpolation and (b) a simple linear regression model using functions in the loadflex package. The red points and green line stand for observations and concentration predictions, respectively.

2.4. Variation Partitioning: PCA, RDA and pRDA

To tackle collinearity issues, many researchers have used principal components analysis (PCA) to reduce a number of correlated variables into a set of uncorrelated variables, which reserves its total variance and uncovers its hidden patterns [28]. In addition, in order to realize the relative importance of different explanatory variables and their interactive effects, direct gradient analysis such as redundancy analysis (RDA) and its successive partial constrained ordinations, i.e., partial RDA (pRDA) have been commonly proposed [18,19]. This allows researchers to explore the relationships between predictor variables and dependent variables by removing the intertwined effects among them [29]. However, most previous studies utilized PCA or RDA methods focusing on the relationship between biological phenomena and environmental influence, and there are only a few studies on water quality (e.g., [30]). Therefore, exploring the likely collinear controlling factors and their internal relationships to riverine DIN transport based on PCA and RDA will be valuable.

In order to interpret the spatial and temporal patterns of riverine NO_3^- and NH_4^+ export and unravel the dependency among controlling factors, i.e., the human disturbance, climatic factors and landscape settings (Table 1), the whole analysis was carried out in three steps [29]: (i) the PCA was applied to find out a set of uncorrelated variables, (ii) detailed relations between export and each one of the controlling factors were displayed using a scatterplot matrix, and (iii) the RDA and pRDA were conducted to disentangle the contribution of the major variables.

Table 1. Definition of different variables used in the three dimensions. Abbre. = abbreviation.

Dimension	Variables	Abbre.	Definition	
Climatic Factors	Rainfall (mm)	RDry	Rainfall in dry season of the year	
		RWet	Rainfall in wet season of the year	
	Streamflow (mm)	SFDry	Discharge rate in dry season of the year	
		SFWet	Discharge rate in wet season of the year	
	Temperature ($^{\circ}\text{C}$)	T	The degree of hotness or coldness of environment	
Landscape Settings	Channel length (km)	CL	Total length of the stream channel	
	Longest channel length (km)	LCL	The length of the longest stream channel in watershed	
	Relief	Rel	The difference between the highest and lowest elevations in watershed	
	Area (km^2)	A	Drainage area of watershed	
	Slope (%)		SLP100	The average slope in the 100 m buffer zone
			SLP200	The average slope in the 200 m buffer zone
			SLP500	The average slope in the 500 m buffer zone
			SLP1000	The average slope in the 1000 m buffer zone
			SLP2000	The average slope in the 2000 m buffer zone
	Drainage density (km^{-1})	SLP	The average slope in watershed	
L/G (m)	DD	Total channel length over drainage area		
Human Disturbances	Population density (population km^{-2})		The ratio of median flow path length to median flow path gradient	
		PD100	Population density in the 100 m buffer zone	
		PD200	Population density in the 200 m buffer zone	
		PD500	Population density in the 500 m buffer zone	
		PD1000	Population density in the 1000 m buffer zone	
		PD2000	Population density in the 2000 m buffer zone	
PD	Population density in watershed			

Table 1. Cont.

Dimension	Variables	Abbre.	Definition
Buildup (%)		BD100	The percentage of buildup area in the 100 m buffer zone
		BD200	The percentage of buildup area in the 200 m buffer zone
		BD500	The percentage of buildup area in the 500 m buffer zone
		BD1000	The percentage of buildup area in the 1000 m buffer zone
		BD2000	The percentage of buildup area in the 2000 m buffer zone
		BD	The percentage of the buildup area in watershed
Agriculture (%)		AGR100	The percentage of agriculture in the 100 m buffer zone
		AGR200	The percentage of agriculture in the 200 m buffer zone
		AGR500	The percentage of agriculture in the 500 m buffer zone
		AGR1000	The percentage of agriculture in the 1000 m buffer zone
		AGR2000	The percentage of agriculture in the 2000 m buffer zone
		AGR	The percentage of the agriculture in the watershed

PCA was applied to reduce redundant information and to transform the original correlated data into another set of uncorrelated variables. The PCA keeps only a few independent sets (patterns) of environmental data that are distinct from each other, which will help to realize the effects of various characteristics of watersheds on NO_3^- and NH_4^+ exports in our study [29,31]. The varimax rotation was selected to better separate divergent groups of variables, as suggested [32]. The environmental variables were centered and standardized in order to approximate normally distributed random errors and then were derived from the PCs via a standardized linear projection which maximizes the variance in the projected space [33]. For a set of observed-dimensional data vectors, $\{t_n\}$, $n \in \{1, \dots, N\}$, the q principal axes $\{w_j\}$, $j \in \{1, \dots, q\}$, could be derived as the orthonormal axes onto which the retained variance under projection is maximal. It can be shown that the vectors w_j are given by the q dominant eigenvectors (i.e., those with the largest associated eigenvalues λ_j) of the sample covariance matrix. The outcomes of PCA help us to identify relationships between these variables and determine which variables require further investigation. The variables with loading higher than 0.1 in the first and second PCs were kept for the following RDA and pRDA analysis to constrain the ordination of environmental variables and to avoid the collinearity problem [31,34].

Moreover, we know water quality is regulated by riparian zones along the river and stream networks, but what needs to be clarified is spatially to what extent their individual effect is [35]. Here, we delineated the buffer zones of 100, 200, 500, 1000 and 2000 m along the stream network using the buffer tool in ArcGIS v.10.7. (ESRI Inc., Redlands, CA, USA) The environmental variables within the entire watershed and five buffer zones were also retrieved as previous studies suggested [30,36,37]. The land cover/land use data were acquired from the Ministry of the Interior of Taiwan (Figure 1b; <https://www.moi.gov.tw>), and the digital elevation model (DEM) data were derived from the open data platform in Taiwan (<https://data.gov.tw/>), which were provided as input for calculations of landscape settings and human disturbance variables (Table 1).

The RDA and pRDA were further applied to quantify the individual effect and integrative contribution among human disturbance, climatic factors and landscape setting on riverine NO_3^- and NH_4^+ exports [18]. RDA extends the algorithm of PCA with a response matrix Y (with n objects and p variables) by an explanatory matrix X (with n objects and m variables). First, RDA produces a matrix of fitted values \hat{Y} through Equation (2),

$$\hat{Y} = X[X^T X]^{-1} X^T Y, \quad (2)$$

and second, runs a PCA based on \hat{Y} [38].

For pRDA, the additional explanatory variables, called covariables, are assembled in matrix W ; the linear effects of the explanatory variables in X on the response variables in Y are adjusted for the effects of the covariables in W [39]. In our study, the total variance of riverine NO_3^- and NH_4^+ exports could be explained by the variables derived from human disturbance, climatic factors and landscape setting,

and their individual contribution of NO_3^- and NH_4^+ export can be finally figured out. We further partitioned the total variation of the riverine NO_3^- and NH_4^+ response variables using three steps (Table 2). First, canonical ordination with no covariables was used to estimate the total amount of variance explained (as sum of canonical eigenvalues) in the NO_3^- and NH_4^+ export attributed to all explanatory variables, human disturbances (H), climatic factors (C) and landscape setting (L), and the total unexplained variance (1–HCL). Second, the combinations of various covariables were considered to calculate the separate effect of each variable (H, C or L), in which an individual predictor variable was run (e.g., H) with the remaining other two as covariables (e.g., C&L). Third, a series of partial canonical ordinations were used to calculate the unique and interactive effects for each set of predictors (e.g., C&L–H) by considering the interaction term of interest as explanatory (C&L) and excluding the effect of not interest (e.g., H). For more details of calculations, please refer to related studies [19,29].

Table 2. Eigenvalues of partial RDA (pRDA) of NO_3^- and NH_4^+ and separate climatic (C), landscape setting (L) and human disturbance (H) and interactive effects among C, L and H.

Environmental Factor	Covariable	$\lambda_{\text{NO}_3^-}$		$\lambda_{\text{NH}_4^+}$	
		Wet	Dry	Wet	Dry
Unexplained variable		0.27	0.14	0.31	0.21
CLH	None	0.73	0.86	0.69	0.79
C	L&H	0.31	0.27	0.03	0.02
L&H	C	0.44	0.27	0.68	0.77
L	C&H	0.00	0.00	0.05	0.00
C&H	L	0.41	0.74	0.06	0.18
H	C&L	0.07	0.09	0.02	0.13
C&L	H	0.31	0.2	0.08	0.02

3. Results

3.1. Riverine DIN Concentration and Export

The mean DIN concentration is 1.66 mg-N L^{-1} , ranging from 0.28 to 8.91 mg-N L^{-1} , while the mean NO_3^- concentration is 0.98 mg-N L^{-1} , varying from 0.26 to 2.79 mg-N L^{-1} , and the mean NH_4^+ concentration is 0.56 mg-N L^{-1} , in the range of 0.01 – 4.59 mg-N L^{-1} . Generally, the mean NO_3^- concentration is higher in the wet season (1.03 mg-N L^{-1}) than in the dry season (0.79 mg-N L^{-1}). In contrast, the mean DIN and NH_4^+ concentrations have higher values in the dry season (1.82 and 0.95 mg-N L^{-1}) than in the wet season (1.66 and 0.48 mg-N L^{-1}) (Table 3, Tables S2 and S3). The annual mean DIN export of 43 watersheds island-wide is $3100 \text{ kg-N km}^{-2} \text{ yr}^{-1}$, ranging from 230 to $10,000 \text{ kg-N km}^{-2} \text{ yr}^{-1}$ (Figure 3 and Table 3), in which the highest DIN export (site 16) reaches over 40-fold of the lowest one (site 39; Tables S4 and S5). Generally, watersheds with high DIN, NO_3^- and NH_4^+ concentrations/exports locate in northern and southwestern Taiwan, while watersheds with relatively low DIN, NO_3^- and NH_4^+ concentrations/exports are those in central and eastern Taiwan. However, high NO_3^- export does not always correspond to high NH_4^+ export (e.g., site 41) (Figure 3, Tables S4 and S5). Meanwhile, DIN exports present a significant seasonality that the wet season (from May to October) can contribute over 75% of the annual export on average, and the NO_3^- and NH_4^+ exports during wet and dry seasons also account for 70–80% and 20–30% of annual DIN exports respectively (Tables S4 and S5). However, the contributions of NO_3^- and NH_4^+ for wet and dry seasons to annual DIN export varied among watersheds. For example, the lowest DIN export is $227 \text{ kg-N km}^{-2} \text{ yr}^{-1}$ in site 39, a relatively pristine watershed (87% of forest cover), and the contributions of NO_3^- and NH_4^+ exports in the wet (dry) season to annual DIN export are both 90% (10%). In contrast, the highest DIN export, $10,228 \text{ kg-N km}^{-2} \text{ yr}^{-1}$, appears in site 16, a more disturbed watershed (65% of agricultural land cover), and the contributions of the NO_3^- and NH_4^+ exports in the wet (dry) season to annual DIN export are 85% (15%) and 55% (45%) (Tables S4 and S5).

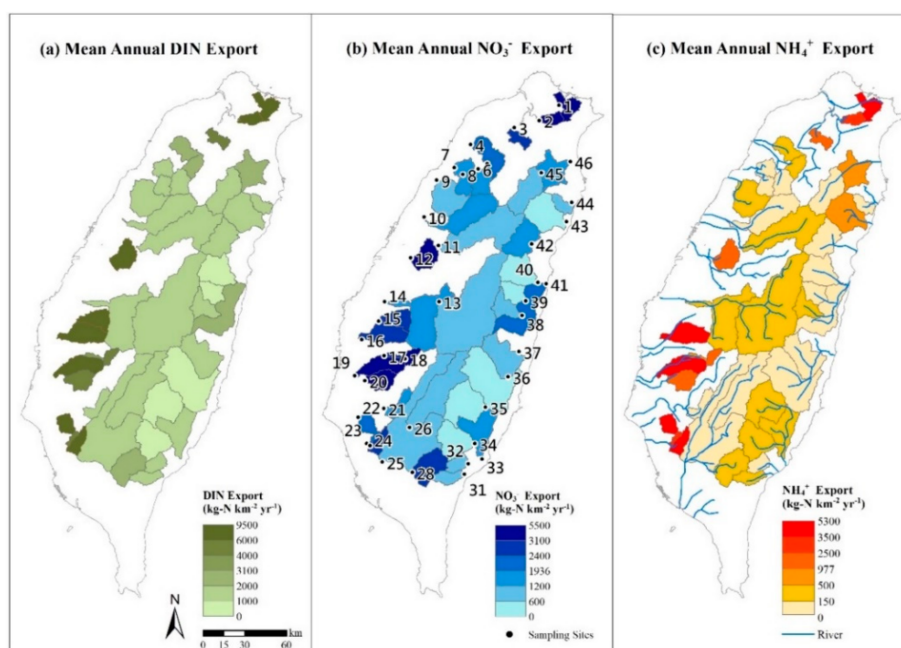


Figure 3. The spatial patterns of DIN (a), NO_3^- (b) and NH_4^+ (c) exports of 43 watersheds. The numbers in panel (b) indicate the sampling sites.

Table 3. Mean estimated seasonal NO_3^- , NH_4^+ and dissolved inorganic nitrogen (DIN) concentrations and exports for 43 sampling sites in the study period (unit: mg-N L^{-1} for conc. and $\text{kg-N km}^{-2} \text{yr}^{-1}$ for flux).

	Annual		Dry Season		Wet Season	
	Conc.	Flux	Conc.	Flux	Conc.	Flux
NO_3^-						
Mean (\pm SD)	0.98 (\pm 0.59)	1936 (\pm 1363)	0.79 (\pm 0.51)	429 (\pm 520)	1.03 (\pm 0.66)	1507 (\pm 1085)
Min-Max	0.26–2.79	212–5801	0.14–2.19	7–2917	0.25–3.58	158–4908
NH_4^+						
Mean (\pm SD)	0.56 (\pm 0.96)	977 (\pm 1456)	0.95 (\pm 1.73)	333 (\pm 551)	0.48 (\pm 0.81)	644 (\pm 950)
Min-Max	0.01–4.59	9–5757	0.01–9.13	1–2372	0.01–3.81	7–3942
DIN						
Mean (\pm SD)	1.66 (\pm 1.69)	3100 (\pm 2827)	1.82 (\pm 2.07)	798 (\pm 982)	1.66 (\pm 1.74)	2303 (\pm 2041)
Min-Max	0.28–8.91	227–10,229	0.16–9.74	8–4730	0.28–10.45	185–7527

The compositions of NO_3^- and NH_4^+ between pristine and disturbed watershed (forest cover <50%) varied as well. For instance, in relatively pristine watersheds, such as site 38 (Figure 4a), NO_3^- exports were generally higher (~70%) than NH_4^+ (~20%). On the contrary, NH_4^+ exports can reach 40% of annual DIN in the higher disturbed watersheds with a smaller drainage area (<1000 km^2) and steep slopes (>30%), such as site 1 (Figure 4b). In addition, some watersheds with higher NH_4^+ exports in lieu of NO_3^- are scattered in the plain (slope < 20%) in southwestern Taiwan, such as sites 15, 16 and 22 (Figure 3, Tables S4 and S5).

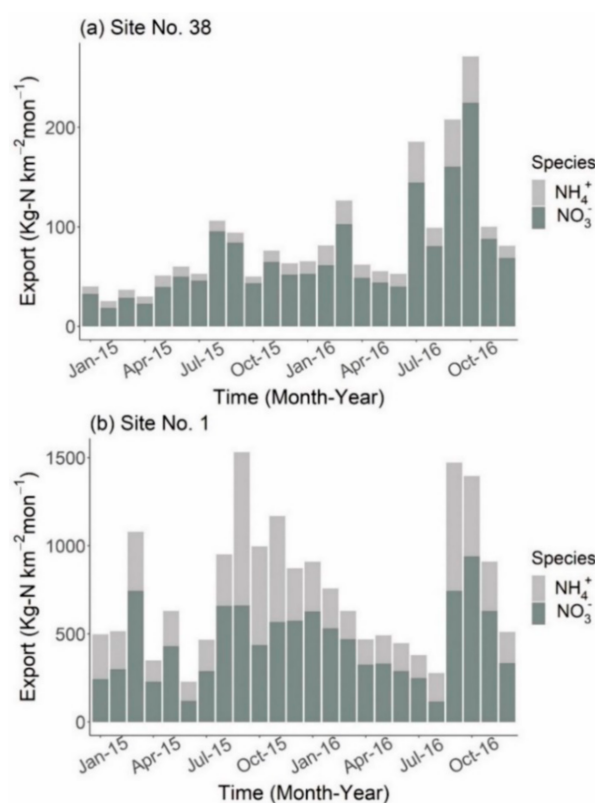


Figure 4. The monthly NO_3^- and NH_4^+ exports in site no. 38 (a) and no. 1 (b) during the study period.

The average DIN export in 2016 ($3460 \text{ kg-N km}^{-2} \text{ yr}^{-1}$) was higher than that in 2015 ($2723 \text{ kg-N km}^{-2} \text{ yr}^{-1}$) due to much higher rainfall, 3480 mm in 2016 compared to 2331 mm in 2015 (Tables S4 and S5). The mean NO_3^- export in 2016 ($2301 \text{ kg-N km}^{-2} \text{ yr}^{-1}$) was higher than in 2015 ($1553 \text{ kg-N km}^{-2} \text{ yr}^{-1}$), whereas the mean NH_4^+ export in 2016 ($940 \text{ kg-N km}^{-2} \text{ yr}^{-1}$) was slightly lower than 2015 ($1016 \text{ kg-N km}^{-2} \text{ yr}^{-1}$), in which most of the decreased NH_4^+ exports appeared in watersheds in northern Taiwan, while some NH_4^+ exports increased in watersheds in southern and eastern Taiwan (Tables S4 and S5).

3.2. Scatterplot Matrix

The correlations between nutrient exports and variables at different buffer zones show that significantly higher coefficients are generally found between annual and seasonal nutrient exports and variables at watershed scale (Figures S1–S3), whereas the fraction of buildup area within a 100 m buffer has higher correlations to DIN ($r = 0.82, p < 0.01$) in the dry season than other variables among different buffer zones (Figure S3). Streamflow, the fraction of agricultural land cover of the entire watershed, buildup area within a 100 m buffer zone and buildup area of the entire watershed show significant positive relationships to DIN export ($r = 0.52\text{--}0.64, p < 0.01$; Figure 5). However, there is a negative relationship found between DIN and slope of entire watershed ($r = -0.64, p < 0.01$; Figure 5).

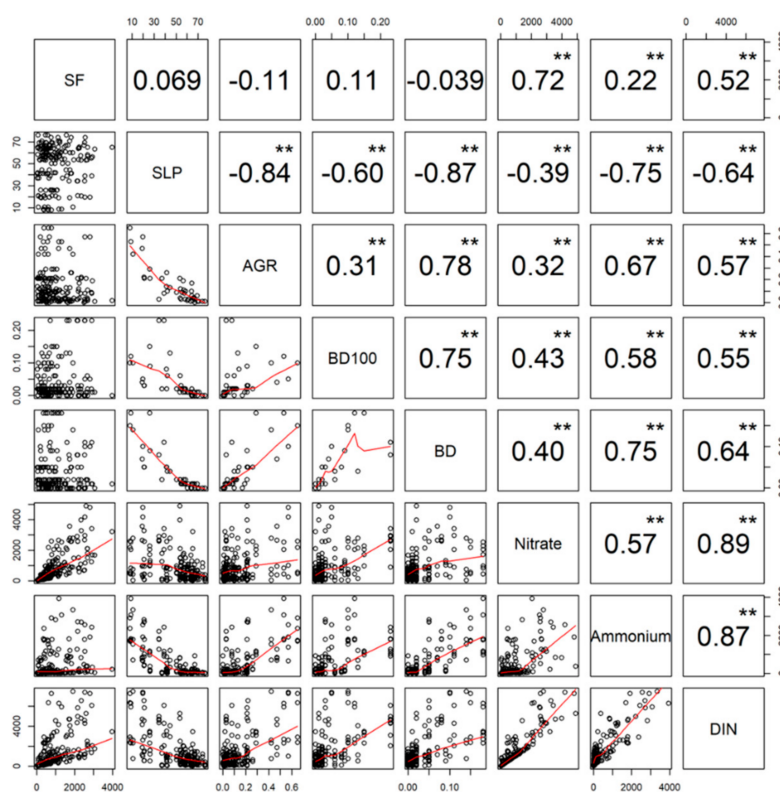


Figure 5. Scatterplot matrix among relative streamflow [SF; mm], slope at watershed scale [SLP; %], the proportion of agriculture at watershed scale [AGR; %], the proportion of buildup in 100 m buffer zone [BD100; %], the proportion of buildup at watershed scale [BD; %], NO_3^- , NH_4^+ , and DIN exports based on all sampling sites. The asterisk indicates that the correlation is statistically significant (p -value: ** < 0.01), and the red lines indicate smooth transition regressions.

Streamflow positively correlates to NO_3^- ($r = 0.72$, $p < 0.01$) and NH_4^+ ($r = 0.22$, $p < 0.01$; Figure 5). The exports of the two ions also significantly correlate to agriculture, buildup area in a 100 m buffer zone and buildup area within the entire watershed, of which the correlation coefficients are higher in NH_4^+ ($r = 0.58$ – 0.75 , $p < 0.01$; Figure 5) than in NO_3^- ($r = 0.32$ – 0.43 , $p < 0.01$; Figure 5). However, the slope is negatively significantly related to NO_3^- exports ($r = -0.39$, $p < 0.01$), NH_4^+ exports ($r = -0.75$, $p < 0.01$), agriculture ($r = -0.84$, $p < 0.01$), buildup area within the 100 m buffer zone ($r = -0.60$, $p < 0.01$) and buildup area within the entire watershed ($r = -0.87$, $p < 0.01$; Figure 5). There are positive correlations among variables of landcover ($r = 0.31$ – 0.78 , $p < 0.01$; Figure 5).

3.3. PCA of Environmental Variables

The first two principal components with eigenvalues > 5.0 are retained, accounting for 70.6% and 72.5% of variances on NO_3^- and NH_4^+ exports, respectively (Figure 6). The combinations of variables within the watershed scale (SF, SLP, AGR, and BD) and buildup area in a 100 m buffer (BD100) can explain much more variances of NO_3^- and NH_4^+ exports than the performance using variables derived from the separate buffer zones ($\leq 60\%$; Figure S4). Generally, the spatial variability of buildup (BD) and slope (SLP) are the main ingredients of the first PCs for NO_3^- and NH_4^+ (Figure 6). The second PC is associated with seasonal variables, i.e., streamflow (SF_{Wet} and SF_{Dry}) and rainfall (RW_{et} and RD_{ry}) during wet and dry periods. Most environmental variables displayed positive correlations with these two response variables (NO_3^- and NH_4^+), except for landscape setting variables such as area (A), channel length (CL), longest channel length (LCL), relief (R) and slope (SLP), i.e., the opposite direction to NO_3^- and NH_4^+ export (blue lines in Figure 6). During the wet season, the smaller projected angle is between the fraction of BD and NO_3^- export (Ni_{Wet}), indicating high relevance between

human impact and the wet season NO_3^- export, while during the dry season, NO_3^- export relates to the vectors dominated by streamflow and rainfall. However, unlike NO_3^- export, NH_4^+ export is dominated by BD regardless of the different seasons. According to the results derived from PCA, five environmental variables including streamflow, slope, the fraction of agricultural land cover, buildup area within a 100 m buffer zone and buildup area of the entire watershed with higher loading were selected for further analysis.

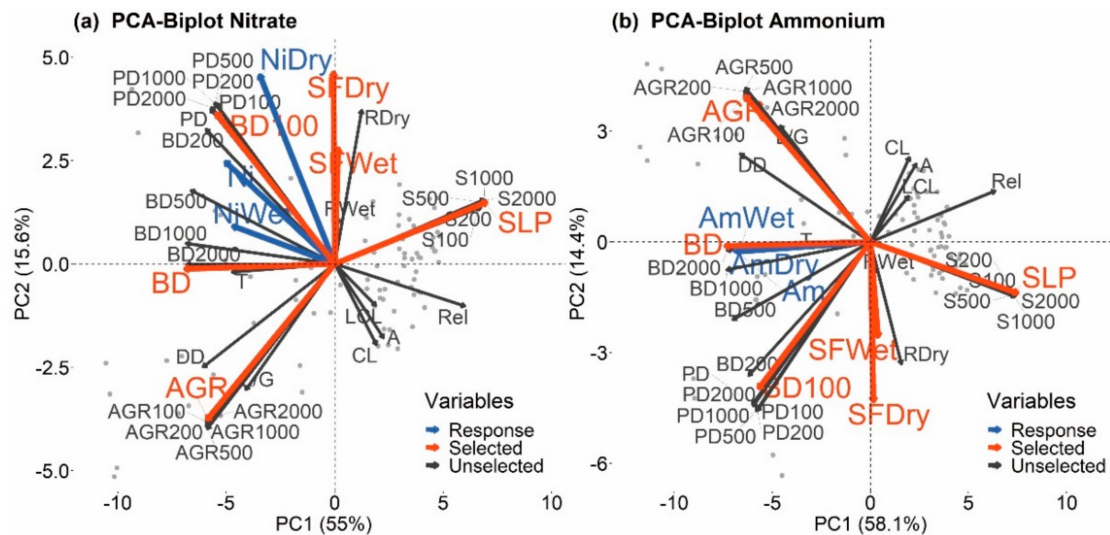


Figure 6. Principal components analysis of environmental variables for 43 catchments (gray dots) for NO_3^- (a) and NH_4^+ export (b). Red-labeled variables are main components for PC1 and PC2. Blue-labeled variables indicate annual nitrate (Ni), dry season nitrate (NiDry) and wet season nitrate export (NiWet) in (a) and annual ammonium (Am), dry season ammonium (AmDry) and wet season ammonium export (AmWet) in (b).

3.4. Variance Partitioning—RDA and pRDA

The RDA model shows that the total variance explained (total inertia) by five selected environmental variables is always higher on NO_3^- exports than on NH_4^+ exports. These predictor variables can explain 86% and 79% of the total variance of NO_3^- and NH_4^+ exports, respectively, in the dry season, but only 73% and 69% in the wet season (Table 4).

Table 4. The marginal effects (λ_1) and total inertia (total effects) of climatic, landscape setting and human disturbance variables on NO_3^- and NH_4^+ exports based on 43 sampling sites.

Species	NO_3^-			NH_4^+		
	Annual	Wet	Dry	Annual	Wet	Dry
	λ_1	λ_1	λ_1	λ_1	λ_1	λ_1
Climatic						
Streamflow (mm)	0.52 **	0.28 **	0.59 **	0.05 **	0.01 ns	0.02 ns
Landscape setting						
Slope (%)	0.15 **	0.32 **	0.12 **	0.56 **	0.64 **	0.61 **
Human disturbance						
Agri. (%)	0.11 **	0.31 **	0.01 ns	0.44 **	0.47 **	0.53 **
Buildup_100 m (%)	0.18 **	0.19 **	0.57 **	0.33 **	0.32 **	0.46 **
Buildup (%)	0.16 **	0.26 **	0.21 **	0.57 **	0.58 **	0.73 **
Total inertial	0.74	0.73	0.86	0.68	0.69	0.79

** $p < 0.01$. ns: not significant.

Streamflow reveals the highest marginal effects on NO_3^- exports, where marginal effects λ_1 increase from 0.28 in the wet season, 0.52 in annual export, to 0.59 in the dry season. However, the effects of streamflow are low ($\lambda_1 < 0.05$) for NH_4^+ annual and seasonal exports (Table 4). In contrast, slope has lower marginal effects on annual and seasonal NO_3^- exports ($\lambda_1 = 0.12\text{--}0.32$) than on NH_4^+ exports ($\lambda_1 = 0.56\text{--}0.64$), and the marginal effects of slope are higher in the wet season ($\lambda_1 = 0.32\text{--}0.64$) than in the dry season ($\lambda_1 = 0.12\text{--}0.61$) for nutrient export (Table 4). The anthropogenic factors, including the fraction of agricultural land cover, buildup area within a 100 m buffer and buildup area of the entire watershed, show higher marginal effects on annual and seasonal NH_4^+ exports ($\lambda_1 = 0.32\text{--}0.73$) than NO_3^- exports ($\lambda_1 = 0.01\text{--}0.57$), except for fraction of buildup area within a 100 m buffer in the dry season on NO_3^- exports (Table 4). Generally, buildup area within a 100 m buffer zone has higher marginal effects on NO_3^- exports ($\lambda_1 = 0.18\text{--}0.57$) than buildup area of entire watershed ($\lambda_1 = 0.16\text{--}0.26$), although the effect of buildup area within a 100 m buffer is slightly lower ($\lambda_1 = 0.19$) than buildup area of entire watershed ($\lambda_1 = 0.26$) in the wet season. In the dry season, the effect of buildup area within a 100 m buffer is 2.5 times ($\lambda_1 = 0.57$) that of buildup area of entire watershed ($\lambda_1 = 0.21$). For NH_4^+ exports, buildup area of entire watershed has the highest effects ($\lambda_1 = 0.57\text{--}0.73$) compared with agriculture ($\lambda_1 = 0.44\text{--}0.53$) and buildup area within a 100 m buffer ($\lambda_1 = 0.32\text{--}0.46$; Table 4).

For NO_3^- exports in pRDA, the lowest (highest) eigenvalue of pure effect on a single variable included is the landscape (climatic) variable in the wet season, 0.003 (0.31), and in the dry season, 0.004 (0.27) (Figure 7). The climatic variable (C) seems to be the dominant factor regarding seasonal NO_3^- exports. It is responsible for over 42% and 31% of variance for wet and dry seasonal NO_3^- exports (Figure 7). The combination of landscape with human disturbance variables (LH) will contribute a significant effect on NO_3^- export in the wet season (0.38 of eigenvalue and 51.59% of explained variance), but decreases substantially in the dry season (0.17 of eigenvalue and 20.00% of explained variance) (Figure 7). While the effects of the combination of climatic with human disturbance variables (CH) increase from 0.04 (5.32% of explained variance) in the wet season (Figure 7a) to 0.38 (44.15% of explained variance) in the dry season (Figure 7b).

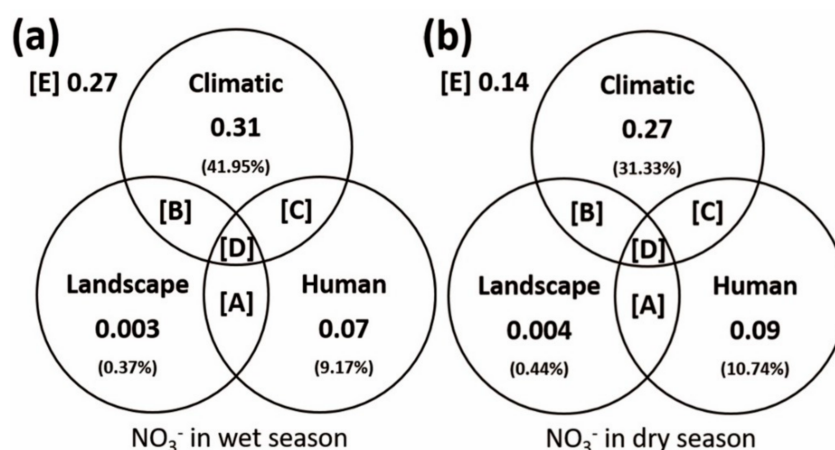


Figure 7. Variance decomposition (conditional effects) of NO_3^- exports in wet (a) and dry (b) seasons in 43 watersheds. Each circle and the intersections indicate the individual effect of climatic [C], landscape (L) and human disturbance (H) variables and their interactive effects on NO_3^- export from pRDA, including the shared variance of landscape setting and human disturbance (LH) [A], landscape setting and climatic variables (LC) [B], climatic variables and human disturbance (CH) [C], among three variables (CLH) [D], and residual variance [E]. In Panel (a): [A] = 0.38 (51.59%); [B] = -0.002 (-0.29%); [C] = 0.04 (5.32%); [D] = -0.06 (-8.09%). In Panel (b): [A] = 0.17 (20.00%); [B] = -0.004 (-0.43%); [C] = 0.38 (44.15%); [D] = -0.05 (-6.22%). The percentage of explained variation of variables is equal to the eigenvalue divided by total inertia.

For NH_4^+ exports in pRDA, the eigenvalues of each single variable (pure effect) are lower than 0.05 (Figure 8). The only exception is the pure effect on human disturbance variables in the dry season ($H = 0.13$), which accounts for 16.4% of explained variance (Figure 8). The dominant effect is the combination of landscape with human disturbance variables (LH) in which eigenvalues reach 0.61 (88.5%) and 0.64 (80.7%) of the total NH_4^+ export variance in the wet and dry season, respectively (Figure 8). Other interactive effects are much lower than LH in both seasons.

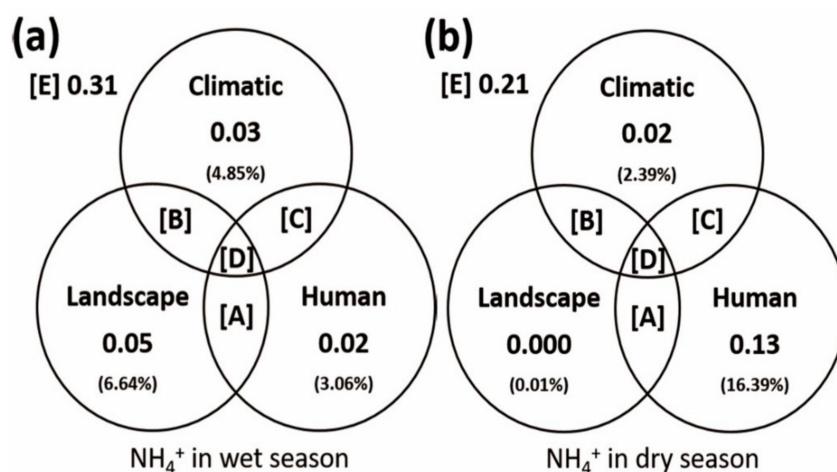


Figure 8. Variance decomposition (conditional effects) of NH_4^+ exports in wet (a) and dry (b) seasons in 43 watersheds. Each circle and the intersections indicate the individual effect of climatic [C], landscape (L) and human disturbance (H) variables and their interactive effects on NH_4^+ export from pRDA, including the shared variance of landscape setting and human disturbance (LH) [A], landscape setting and climatic variables (LC) [B], climatic variables and human disturbance (CH) [C], among three variables (CLH) [D], and residual variance [E]. In Panel (a): [A] = 0.61 (88.54%); [B] = -0.004 (-0.56%); [C] = 0.001 (0.09%); [D] = -0.02 (-2.62%). In Panel (b): [A] = 0.64 (80.70%); [B] = 0.001 (0.08%); [C] = 0.03 (4.10%); [D] = -0.03 (-3.67%). The percentage of explained variation of variables is equal to the eigenvalue divided by total inertia.

4. Discussion

4.1. Characteristics of DIN Concentrations and Exports in Taiwan

On average, DIN concentration from 43 island-wide watersheds across Taiwan is 1.66 mg-N L^{-1} , and the two main DIN species present a mediated dilution effect with streamflow (Table 3 and Figure S5). The average riverine DIN export reaches $3100 \text{ kg-N km}^{-2} \text{ yr}^{-1}$, which is much greater than the global mean ($208 \text{ kg-N km}^{-2} \text{ yr}^{-1}$) [12]. High rainfall and streamflow, N deposition and N fertilizer application for agricultural production at upstream regions can account for the significant nutrients streamflow [11]. The results reveal that DIN export and concentration vary spatially, ranging from $200 \text{ kg-N km}^{-2} \text{ yr}^{-1}$, 0.3 mg-N L^{-1} in less disturbed watersheds (site 39; Figure 3), to over $10,000 \text{ kg-N km}^{-2} \text{ yr}^{-1}$, 8.8 mg-N L^{-1} in highly disturbed watersheds (site 16; Figure 3). The spatial DIN surge also indicates that the environmental background actually exports DIN and consequently induces the risk of eutrophication in the downstream. Previous studies suggested that intact forested watersheds demonstrated high N retention capacity but the capacity would collapse with significant land cover conversion [16,40]. In our study, higher NH_4^+ exports in highly disturbed watersheds with smaller drainage area ($<1000 \text{ km}^2$) and steep slope ($>30\%$) show that these environmental backgrounds are unfavorable to ammonia oxidation or assimilation due to rapid transport [41]. In addition, most of the watersheds with higher NH_4^+ exports than NO_3^- appear in plain areas where human disturbances are high and sewage systems are deficient [42].

The island-wide DIN estimation reveals that the wet season (May to October) contributes 78% of the annual DIN export, $3100 \text{ kg-N km}^{-2} \text{ yr}^{-1}$, which is consistent with previous findings that hydrological processes control DIN export [43,44]. Because nutrient export and transport is regulated by precipitation and streamflow, this controlling factor is more dominant in the tropics and subtropics [12,45]. The torrential rainfall brought by typhoons during the humid growing summer in Taiwan accounts for 30–50% of the annual precipitation, 2500 mm yr^{-1} [13,46], and consequently causes vital effects on biogeochemical processes, i.e., a huge amount of nutrients being flushed out from terrestrial ecosystems to aquatic ecosystems. It also explains why the nutrient streamflow in Taiwan is in the leading place worldwide [12].

4.2. Influences of Main Variables and Their Interactive Effects on DIN Export

4.2.1. Climatic Control

In tropical/subtropical mountainous Taiwan, abundant rainfall usually leads to a great amount of net nutrient exports even during the growing summer, which is distinct from the findings in temperate forest ecosystems [11,45,47]. Water is the conveyor of ion movement. In spite of the dilution of NO_3^- concentration during flood periods (wet season), the extensive runoff by typhoons flushes over surface and near-surface and leads to greater DIN exports [13].

The relation between export and streamflow (F-Q relation), which definitely shows export change with streamflow, is particularly crucial as regarding nutrient balance and transport, although the F-Q relation, which inevitably incorporates streamflow in the calculation, could likely lead to the “spurious relation”. However, the F-Q relation, which can present the dominance of supply-limited or kinetically-limited under different hydrologic conditions, helps to indicate the nutrient budget balance, and the transported amount is also important. Notably, there are totally different hydrological controls on NO_3^- and NH_4^+ transport. One is that streamflow plays a strong role on NO_3^- export ($r = 0.72$; $\lambda_1 = 0.28\text{--}0.59$), which is in contrast to a relatively weak relation with NH_4^+ export ($r = 0.22$; $\lambda_1 < 0.05$). The positive NO_3^- streamflow relation indicates the sources are relatively sufficient, as compared to kinetic transport. One possible interpretation is that warmer and more humid conditions (e.g., higher soil moisture) during the wet summer season are favorable for nitrification and promotes NO_3^- accumulation and then transports it from the soil to the aquatic system [48,49]. On the contrary, NH_4^+ is easily converted and emitted to the atmosphere via microbial activities in warm and humid conditions [15,50], which has lower retention in soil capacity compared to NO_3^- . Whether NH_4^+ is source-limited casts a shadow of doubt on hydrologic control on NH_4^+ transport.

4.2.2. The Consideration of Landscape and Buffer Zone

Streams receive nutrients from aquatic ecosystems and adjacent terrestrial landscapes, such that landscape configuration at watershed- or buffer zone-scale has important influences on stream water quality, ecological process and biodiversity. Watersheds with steeper slopes usually export more nutrients [51], yet our results surprisingly show that slope is negatively related to NO_3^- and NH_4^+ exports (Figure 5). The possible reason is that most upstream watersheds with steep slopes are covered by pristine forests where anthropogenic sources are scarce [10,52]. Studies suggested that elevation might be a suitable parameter to predict water quality [30], but the collinearity between landscape (e.g., elevation or SLP) and human-made land cover (e.g., AGR and BD) from the high, steep montane region to the low, flat plain in Taiwan keeps us from using both simultaneously, even they might have significant contribution on nutrient exports.

Many studies demonstrate the control of land use and landscape on water quality at watershed scale [28,30], but few studies consider the distance from source area to river, i.e., the regulation of the riparian or buffer zone on nutrient movement. Plants and microbial activities within the riparian zone can help to uptake a great quantity of water, nutrients and sediments, mitigating the nutrients export to aquatic ecosystems within the watershed [53,54]. However, the effective buffer distance

is uncertain, and it could vary with the elements which are concerned [36,55]. A study conducted in Puerto Rico examined how the landscape pattern changes affected water quality in-stream and found that turbidity and dissolved oxygen responded to land use and land cover (LUC) at watershed scale [35], phosphorus concentration and fecal matter responded to LUC at sub-watershed scale, whereas nitrogen concentrations linked to LUC in riparian buffers of larger watersheds [35]. Another study conducted in the Saginaw Bay of central Michigan investigating 62 catchments with a gradient of disturbed land cover showed that the land use factors within a 100 m buffer zone adjacent to the river could explain much higher (or equal) variance of NO_3^- and NH_4^+ concentrations than those derived from the watershed scale [52]. Conversely, the relationships between total nitrogen exports and land use at the watershed scale were better than riparian buffer zones of 200 and 400 m in highly disturbed rivers in Illinois and Texas [56]. Previous assessments, based upon mountainous background, demonstrated that the buffer zone within a 100 m riparian zone, the buildup area particularly, plays an important role in regulating DIN exports [56–58]. In Taiwan, the deficiency of sewage systems in buildup areas located near river networks contributes a significant amount to the DIN exports [42]. The percentage of buildup at the watershed scale highlighted in our study indicates that dispersal non-point sewage sources in the buildup area and scattered agricultural activities would be critical in assessing NH_4^+ export.

4.2.3. Human Disturbance

The contribution of human activities to DIN exports (including NO_3^- and NH_4^+) from land to water has been underscored due to agricultural activities (e.g., fertilizer application) and urbanization (e.g., domestic wastewater) [52,59]. To meet the ever-increasing demand, agricultural activities, such as high value fruit, montane cabbage and tea plantations, are pervasive in mountainous Taiwan. Consequently, the excessive addition of inorganic N fertilizer and organic manure on the thin soil layer is readily flushed out to aquatic ecosystems downstream during wet season [12,60]. The N retention or removal capacity within watersheds will dramatically decrease if forests are transformed to agricultural areas [61]. However, though the effects of agricultural land on NO_3^- and NH_4^+ exports are statistically significant, their contributions are weaker than previous studies suggested [57,58]. A Canadian study suggested that urban land use has a stronger effect on water quality than agriculture has [14]. Obviously, the importance of agricultural and urban land use on DIN exports is not easy to identify and separate, not only due to the area, but also the “intensity” (e.g., intensive agriculture or dense population) and spatial configuration. For example, the effect of urban areas is minor in Finland, because the population and settlements are mostly scattered so that wastewater can be purified before it flows into main streams [28].

In this study, both NO_3^- and NH_4^+ exports are significantly correlated to AGR and BD, which shows that AGR and BD are important for DIN exports (Figure 5). Notably, higher correlation coefficients of AGR and BD to NH_4^+ export ($r = 0.67\text{--}0.75$) than those to NO_3^- export ($r = 0.32\text{--}0.40$) indicates that land use pattern is more effective to explain the variance of NH_4^+ export. Conceptually, NH_4^+ is easier to be taken up by plants and to be oxidized through nitrification and thus NO_3^- is the main species of DIN within agriculture-dominated catchments. The intensive urban developments located near stream riparian in Taiwan deteriorates water quality directly and contributes a significant amount to the DIN exports. This phenomenon is reflected by the higher effect of BD100 (buildup area in a 100 m buffer zone) than the BD of the entire watershed on NO_3^- export during the dry season (Table 4). Therefore, domestic wastewater inevitably elevates NH_4^+ export, which indicates a strong intrinsic collinearity with agriculture and buildup area. Such intrinsic collinearity presents an inseparable human-landscape system, and their interplay could not be distinguished perfectly.

4.2.4. Interactive Effects among Variables

It was noticeable that interactive effects between landscape and human variables can explain most variabilities of NO_3^- export in the wet season (51.59% of the total variance) and seasonal NH_4^+ export

(both >80% of the total variance). Meanwhile, interactive effects between climatic and human variables explain 44.15% of the total NO_3^- export variance in the dry season. Thus, the interactive effect between landscape setting and human disturbance and climatic and human disturbance will result in a high efficiency of prediction regarding NO_3^- and NH_4^+ export in different conditions. One explanatory variable might be partially linked to other variables and altogether would improve or reduce the predictive power in evaluation of NO_3^- and NH_4^+ export [62]. For example, the opposite influences of streamflow and slope might suppress their capability to assess NO_3^- and NH_4^+ exports without eliminating the collinearity between them. The mixed effects of environmental variables also suggest that it is necessary and will be more effective to apply an integrative management strategy [63].

There is a significant change between the controlling interactive effects of NO_3^- export in the wet and dry seasons. In the wet season, streamflow and interactive effects between landscape setting and human disturbance might reveal that they are two unique groups controlling the variance of NO_3^- export. This might be reasonable because the abundant rainfall during the humid summer will decrease the spatial variability of streamflow across Taiwan, which leads to a weaker relationship between streamflow and the interactive effects of landscape setting and human disturbance. On the contrary, the increase of the interactive effects between climatic and human disturbance might indicate the increasing spatial variability of streamflow in the dry season. Therefore, when we predict NO_3^- export in the wet season, both streamflow and the interactive effects between landscape setting and human disturbance cannot be ignored. Furthermore, the strong interactive effects between landscape setting and human disturbance on NH_4^+ export, indicates that these two groups are the primary control of NH_4^+ export. Because landscape setting and human disturbance are highly related (Figure 5), the variance explained by them might be similar and it might be difficult to separate their individual effect from both combined.

Some critical variables are not included in this study but might be significant in other regions. Studies found a strong negative relationship between nitrogen content and soil type [14]. However, most watersheds in Taiwan cross various soil substrates and geological units, which challenges us to unambiguously define a specific soil type for each watershed. In addition, long-lasting atmospheric nitrogen deposition could lead to N saturation in temperate forest ecosystems, resulting in net loss of nitrate to streams and consequent acidification of stream water [1,16,64]. A large-scale study indicated that riverine N export could be predicted by atmospheric N deposition rates [65]. Therefore, the influence of interaction between atmospheric deposition, land use and hydroclimate should be considered in following syntheses of DIN responses or developing models for riverine DIN export [66].

5. Conclusions

This work identified the major predictor variables and their interactive effects on DIN, NO_3^- and NH_4^+ exports. Totally, 35 predictor variables among climatic, landscape setting and human disturbance dimensions were applied using PCA and pRDA analysis based upon data derived from 43 watersheds island-wide in Taiwan. Generally, the PCA identified that SF, SLP, AGR, BD and BD100 are the main variables which can mostly explain the variances of DIN, NO_3^- and NH_4^+ exports. Because nutrient export is the product of nutrient concentration and streamflow, streamflow, as expected, is the strongest predictor for NO_3^- export ($r = 0.72$), but not for NH_4^+ export, due to active biogeochemical processes. Meanwhile, the SLP ($r = 0.75$) and BD ($r = -0.75$) are equally best correlated to NH_4^+ export. Based on the results of the pRDA model, five selected environmental variables can explain NO_3^- and NH_4^+ export promisingly, but with different interactive effects. For NO_3^- export in the wet season, the climatic variable and human-landscape variables are independently responsive to most variances, while the dependent climatic-human variables present high marginal effects on NO_3^- exports in the dry season. The effective variables shift from human-landscape to climatic-human with seasons showing the mechanistic shift of nutrient transport. For NH_4^+ export, the residual variances are 0.31 and 0.21 for the wet and dry seasons, respectively, and climatic variables (e.g., streamflow) are not effective variables for NH_4^+ transport. The human-landscape variables are the major factors to explain the total

variance of NH_4^+ export (over 80%), in both the wet and dry seasons. The shift of interactive effects of variables on nutrient export is important for water quality management at watershed scale and designing mitigation strategies. Inevitably, the effects of intrinsic collinearity in the human-landscape system cannot be clearly separated due to spurious correlation, though the statistical approach provides some cues. For example, paired AGR and BD or SLP and BD are highly collinear but difficult to single out for estimating nutrient export and for interpretation. Nevertheless, with the accumulation of these studies, it is more possible to clarify the interactive effects, which could be of great help in advancing the understanding of DIN export mechanisms and global synthesized assessment.

Supplementary Materials: The following are available online at <http://www.mdpi.com/2073-4441/12/11/2981/s1>, Table S1: The basic landscape characteristics of the 43 sampling sites, Table S2: Estimated annual and seasonal DIN, NO_3^- and NH_4^+ concentrations for 43 sampling sites in 2015 (unit: mg-N L^{-1}), Table S3: Estimated annual and seasonal DIN, NO_3^- and NH_4^+ concentrations for 43 sampling sites in 2016 (unit: mg-N L^{-1}), Table S4: Estimated annual and seasonal DIN, NO_3^- and NH_4^+ exports for 43 sampling sites in 2015 (unit: $\text{kg-N km}^{-2} \text{ yr}^{-1}$), Table S5: Estimated annual and seasonal DIN, NO_3^- and NH_4^+ exports for 43 sampling sites in 2016 (unit: $\text{kg-N km}^{-2} \text{ yr}^{-1}$). Figure S1: Scatterplot matrix among streamflow [SF; mm], slope [SLP; %], the proportion of agriculture [AGR; %], the proportion of buildup [BD; %] of various scales and annual NO_3^- , and NH_4^+ and DIN exports at (a) 100 m, (b) 200 m, (c) 500 m, (d) 1000 m, (e) 2000 m and (f) entire watershed scales. The asterisk indicates that the correlation is statistically significant (p -value: $** < 0.01$), and the red lines indicate smooth transition regressions, Figure S2: Scatterplot matrix among streamflow [SF; mm], slope [SLP; %], the proportion of agriculture [AGR; %], the proportion of buildup [BD; %] of various scales and NO_3^- (Ni), NH_4^+ (Am) and DIN exports during the wet season at (a) 100 m, (b) 200 m, (c) 500 m, (d) 1000 m, (e) 2000 m and (f) entire watershed scales. The asterisk indicates that the correlation is statistically significant (p -value: $** < 0.01$), and the red lines indicate smooth transition regressions, Figure S3: Scatterplot matrix among streamflow [SF; mm], slope [SLP; %], the proportion of agriculture [AGR; %], the proportion of buildup [BD; %] of various scales and NO_3^- (Ni), NH_4^+ (Am) and DIN exports during the dry season at (a) 100 m, (b) 200 m, (c) 500 m, (d) 1000 m, (e) 2000 m and (f) entire watershed scales. The asterisk indicates that the correlation is statistically significant (p -value: $** < 0.01 < * < 0.05$), and the red lines indicate smooth transition regressions. Figure S4: Principal components analysis of environmental variables for 43 catchments (gray dots) for NO_3^- export (left panel) and NH_4^+ export (right panel) at different buffer zones: (a, b) 100 m, (c, d) 200 m, (e, f) 500 m, (g, h) 1000 m, (i, j) 2000 m and (k, l) entire watershed. Red-labeled variables are main components for PC1 and PC2. Blue-labeled variables indicate annual nitrate (Ni), dry season nitrate (NiDry), and wet season nitrate export (NiWet) in (left panel) and annual ammonium (Am), dry season ammonium (AmDry) and wet season ammonium export (AmWet) in (right panel), Figure S5: The relationship between the observed concentration (y -axis) and the simulated discharge (x -axis) in site no.38 (a) and no.1 (b) during the study period. Obs_NO3 is the observed NO_3^- concentration; Obs_NH4 is the observed NH_4^+ concentration.

Author Contributions: Conceptualization, J.-C.H. and W.-S.L.; formal analysis, W.-S.L.; data curation, S.-C.C., Y.-S.L., C.-S.L., L.-C.L., J.-Y.L., Y.-T.S., M.-C.L., and P.-H.C.; writing—original draft preparation, W.-S.L., C.-T.C., and J.-C.H.; writing—review and editing, C.-T.C. and J.-C.H.; supervision and funding acquisition, J.-C.H. All authors have read and agreed to the published version of the manuscript.

Funding: This research was funded by Taiwan Ministry of Science and Technology and NTU Research Center for Future Earth to J.-C.H. (MOST 109–2621-M–002–003-MY3, MOST 107–2621-B–002–003-MY3 and 107 L901004) and C.-T.C. (MOST 108–2313-B–029–001 and 109–2621-B–029–004).

Acknowledgments: The authors are grateful to the Water Resource Agency and the Ministry of the Interior of Taiwan for providing the hydrological and land cover/land use data.

Conflicts of Interest: The authors declare no conflict of interest.

References

1. Aber, J.; McDowell, W.; Nadelhoffer, K.; Magill, A.; Berntson, G.; Kamakea, M.; McNulty, S.; Currie, W.; Rustad, L.; Fernandez, I. Nitrogen saturation in temperate forest ecosystems: Hypotheses revisited. *Bioscience* **1998**, *48*, 921–934. [[CrossRef](#)]
2. Galloway, J.N.; Dentener, F.J.; Capone, D.G.; Boyer, E.W.; Howarth, R.W.; Seitzinger, S.P.; Asner, G.P.; Cleveland, C.C.; Green, P.; Holland, E.A. Nitrogen cycles: Past, present, and future. *Biogeochemistry* **2004**, *70*, 153–226. [[CrossRef](#)]
3. Seitzinger, S.P.; Mayorga, E.; Bouwman, A.F.; Kroeze, C.; Beusen, A.H.W.; Billen, G.; Van Drecht, G.; Dumont, E.; Fekete, B.M.; Garnier, J.; et al. Global river nutrient export: A scenario analysis of past and future trends. *Glob. Biogeochem. Cycle* **2010**, *24*, GB0A08. [[CrossRef](#)]

4. Rockström, J.; Steffen, W.; Noone, K.; Persson, Å.; Chapin, F.S.; Lambin, E.F.; Lenton, T.M.; Scheffer, M.; Folke, C.; Schellnhuber, H.J. A safe operating space for humanity. *Nature* **2009**, *461*, 472–475. [[CrossRef](#)] [[PubMed](#)]
5. Tørseth, K.; Aas, W.; Breivik, K.; Fjæraa, A.M.; Fiebig, M.; Hjellbrekke, A.-G.; Lund Myhre, C.; Solberg, S.; Yttri, K.E. Introduction to the European Monitoring and Evaluation Programme (EMEP) and observed atmospheric composition change during 1972–2009. *Atmos. Chem. Phys.* **2012**, *12*, 5447–5481. [[CrossRef](#)]
6. Vet, R.; Artz, R.S.; Carou, S.; Shaw, M.; Ro, C.-U.; Aas, W.; Baker, A.; Bowersox, V.C.; Dentener, F.; Galy-Lacaux, C. A global assessment of precipitation chemistry and deposition of sulfur, nitrogen, sea salt, base cations, organic acids, acidity and pH, and phosphorus. *Atmos. Environ.* **2014**, *93*, 3–100. [[CrossRef](#)]
7. Chang, K.-H.; Jeng, F.-T.; Tsai, Y.-L.; Lin, P.-L. Modeling of long-range transport on Taiwan's acid deposition under different weather conditions. *Atmos. Environ.* **2000**, *34*, 3281–3295. [[CrossRef](#)]
8. Conley, D.J.; Paerl, H.W.; Howarth, R.W.; Boesch, D.F.; Seitzinger, S.P.; Havens, K.E.; Lancelot, C.; Likens, G.E. Controlling eutrophication: Nitrogen and phosphorus. *Science* **2009**, *323*, 1014–1015. [[CrossRef](#)]
9. Howarth, R.; Swaney, D.; Billen, G.; Garnier, J.; Hong, B.; Humborg, C.; Johnes, P.; Mörth, C.-M.; Marino, R. Nitrogen fluxes from the landscape are controlled by net anthropogenic nitrogen inputs and by climate. *Front. Ecol. Environ.* **2012**, *10*, 37–43. [[CrossRef](#)]
10. Chang, C.T.; Huang, J.-C.; Wang, L.; Shih, Y.T.; Lin, T.C. Shifts in stream hydrochemistry in responses to typhoon and non-typhoon precipitation. *Biogeosciences* **2018**, *15*, 2379–2391. [[CrossRef](#)]
11. Huang, J.-C.; Lee, T.-Y.; Kao, S.-J.; Hsu, S.-C.; Lin, H.-J.; Peng, T.-R. Land use effect and hydrological control on nitrate yield in subtropical mountainous watersheds. *Hydrol. Earth Syst. Sci.* **2012**, *16*, 699. [[CrossRef](#)]
12. Huang, J.-C.; Lee, T.-Y.; Lin, T.-C.; Hein, T.; Lee, L.-C.; Shih, Y.-T.; Kao, S.-J.; Shiah, F.-K.; Lin, N.-H. Effects of different N sources on riverine DIN export and retention in a subtropical high-standing island, Taiwan. *Biogeosciences* **2016**, *13*, 1787. [[CrossRef](#)] [[PubMed](#)]
13. Lee, T.-Y.; Huang, J.-C.; Kao, S.-J.; Tung, C.-P. Temporal variation of nitrate and phosphate transport in headwater catchments: The hydrological controls and land use alteration. *Biogeosciences* **2013**, *10*, 2617–2632. [[CrossRef](#)]
14. Sliva, L.; Williams, D.D. Buffer zone versus whole catchment approaches to studying land use impact on river water quality. *Water Res.* **2001**, *35*, 3462–3472. [[CrossRef](#)]
15. Pajares, S.; Bohannan, B.J. Ecology of nitrogen fixing, nitrifying, and denitrifying microorganisms in tropical forest soils. *Front. Microbiol.* **2016**, *7*, 1045. [[CrossRef](#)]
16. Howarth, R.W. An assessment of human influences on fluxes of nitrogen from the terrestrial landscape to the estuaries and continental shelves of the North Atlantic Ocean. *Nutr. Cycl. Agroecosyst.* **1998**, *52*, 213–223. [[CrossRef](#)]
17. Graham, M.H. Confronting multicollinearity in ecological multiple regression. *Ecology* **2003**, *84*, 2809–2815. [[CrossRef](#)]
18. Ter Braak, C.J. *CANOCO-a FORTRAN Program. for Canonical Community Ordination by [Partial][Etrended][Canonical] Correspondence Analysis, Principal Components Analysis and Redundancy Analysis (Version 2.1)*; Wageningen University: Wageningen, The Netherlands, 1988.
19. Borcard, D.; Legendre, P.; Drapeau, P. Partialling out the spatial component of ecological variation. *Ecology* **1992**, *73*, 1045–1055. [[CrossRef](#)]
20. Chang, C.-T.; Wang, S.-F.; Vadeboncoeur, M.A.; Lin, T.-C. Relating vegetation dynamics to temperature and precipitation at monthly and annual timescales in Taiwan using MODIS vegetation indices. *Int. J. Remote Sens.* **2014**, *35*, 598–620. [[CrossRef](#)]
21. Parajka, J.; Viglione, A.; Rogger, M.; Salinas, J.L.; Sivapalan, M.; Blöschl, G. Comparative assessment of predictions in ungauged basins—Part 1: Runoff-hydrograph studies. *Hydrol. Earth Syst. Sci.* **2013**, *17*, 1783–1795. [[CrossRef](#)]
22. Huang, J.-C.; Kao, S.-J.; Lin, C.-Y.; Chang, P.-L.; Lee, T.-Y.; Li, M.-H. Effect of subsampling tropical cyclone rainfall on flood hydrograph response in a subtropical mountainous catchment. *J. Hydrol.* **2011**, *409*, 248–261. [[CrossRef](#)]
23. Nash, J.E.; Sutcliffe, J.V. River flow forecasting through conceptual models part I—A discussion of principles. *J. Hydrol.* **1970**, *10*, 282–290. [[CrossRef](#)]
24. Appling, A.P.; Leon, M.C.; McDowell, W.H. Reducing bias and quantifying uncertainty in watershed flux estimates: The R package loadflex. *Ecosphere* **2015**, *6*, 1–25. [[CrossRef](#)]

25. Porterfield, G. *Computation of Fluvial-Sediment Discharge*; US Government Printing Office: Washington, DC, USA, 1972. [[CrossRef](#)]
26. Robertson, D.M.; Roerish, E.D. Influence of various water quality sampling strategies on load estimates for small streams. *Water Resour. Res.* **1999**, *35*, 3747–3759. [[CrossRef](#)]
27. Ferguson, R. River loads underestimated by rating curves. *Water Resour. Res.* **1986**, *22*, 74–76. [[CrossRef](#)]
28. Varanka, S.; Luoto, M. Environmental determinants of water quality in boreal rivers based on partitioning methods. *River Res. Appl.* **2012**, *28*, 1034–1046. [[CrossRef](#)]
29. Liu, Q. Variation partitioning by partial redundancy analysis (RDA). *Environmetrics* **1997**, *8*, 75–85. [[CrossRef](#)]
30. Nava-López, M.Z.; Diemont, S.A.; Hall, M.; Ávila-Akerberg, V. Riparian buffer zone and whole watershed influences on river water Quality: Implications for ecosystem services near megacities. *Environ. Process.* **2016**, *3*, 277–305. [[CrossRef](#)]
31. Johnson, R.K.; Furse, M.T.; Hering, D.; Sandin, L. Ecological relationships between stream communities and spatial scale: Implications for designing catchment-level monitoring programmes. *Freshw. Biol.* **2007**, *52*, 939–958. [[CrossRef](#)]
32. Jolliffe, I.T.; Cadima, J. Principal component analysis: A review and recent developments. *Philos. Trans. R. Soc. A* **2016**, *374*, 20150202. [[CrossRef](#)]
33. Hotelling, H. Analysis of a complex of statistical variables into principal components. *J. Educ. Psychol.* **1933**, *24*, 417. [[CrossRef](#)]
34. Sutter, J.M.; Kalivas, J.H. Comparison of forward selection, backward elimination, and generalized simulated annealing for variable selection. *Microchem. J.* **1993**, *47*, 60–66. [[CrossRef](#)]
35. Uriarte, M.; Yackulic, C.B.; Lim, Y.; Arce-Nazario, J.A. Influence of land use on water quality in a tropical landscape: A multi-scale analysis. *Landsc. Ecol.* **2011**, *26*, 1151. [[CrossRef](#)]
36. Nielsen, A.; Trolle, D.; Søndergaard, M.; Lauridsen, T.L.; Bjerring, R.; Olesen, J.E.; Jeppesen, E. Watershed land use effects on lake water quality in Denmark. *Ecol. Appl.* **2012**, *22*, 1187–1200. [[CrossRef](#)] [[PubMed](#)]
37. Xiao, R.; Wang, G.; Zhang, Q.; Zhang, Z. Multi-scale analysis of relationship between landscape pattern and urban river water quality in different seasons. *Sci. Rep.* **2016**, *6*, 1–10. [[CrossRef](#)] [[PubMed](#)]
38. Legendre, P.; Legendre, L. Chapter 9—Ordination in reduced space. In *Developments in Environmental Modelling*; Legendre, P., Legendre, L., Eds.; Elsevier: Amsterdam, The Netherlands, 2012; Volume 24, pp. 425–520.
39. Legendre, P.; Oksanen, J.; ter Braak, C.J. Testing the significance of canonical axes in redundancy analysis. *Methods Ecol. Evol.* **2011**, *2*, 269–277. [[CrossRef](#)]
40. Groffman, P.M.; Law, N.L.; Belt, K.T.; Band, L.E.; Fisher, G.T. Nitrogen fluxes and retention in urban watershed ecosystems. *Ecosystems* **2004**, *7*, 393–403. [[CrossRef](#)]
41. Halbfuß, S.; Gebel, M.; Bürger, S. Modelling of long term nitrogen retention in surface waters. *Adv. Geosci.* **2010**, *27*, 145–148. [[CrossRef](#)]
42. Lee, T.-Y.; Shih, Y.-T.; Huang, J.-C.; Kao, S.-J.; Shiah, F.-K.; Liu, K.-K. Speciation and dynamics of dissolved inorganic nitrogen export in the Danshui River, Taiwan. *Biogeosciences Discuss.* **2014**, *11*, 5307–5321. [[CrossRef](#)]
43. He, B.; Kanae, S.; Oki, T.; Hirabayashi, Y.; Yamashiki, Y.; Takara, K. Assessment of global nitrogen pollution in rivers using an integrated biogeochemical modeling framework. *Water Res.* **2011**, *45*, 2573–2586. [[CrossRef](#)]
44. Ohowa, B.; Mwashote, B.; Shimbira, W. Dissolved inorganic nutrient fluxes from two seasonal rivers into Gazi Bay, Kenya. *Estuar. Coast. Shelf Sci.* **1997**, *45*, 189–195. [[CrossRef](#)]
45. Chang, C.-T.; Wang, L.-J.; Huang, J.-C.; Liu, C.-P.; Wang, C.-P.; Lin, N.-H.; Wang, L.; Lin, T.-C. Precipitation controls on nutrient budgets in subtropical and tropical forests and the implications under changing climate. *Adv. Water Resour.* **2017**, *103*, 44–50. [[CrossRef](#)]
46. Chang, C.; Hamburg, S.; Hwong, J.; Lin, N.; Hsueh, M.; Chen, M.; Lin, T.-C. Impacts of tropical cyclones on hydrochemistry of a subtropical forest. *Hydrol. Earth Syst. Sci.* **2013**, *17*, 3815. [[CrossRef](#)]
47. Likens, G.E. *Biogeochemistry of a Forested Ecosystem*; Springer: Berlin/Heidelberg, Germany, 2013. [[CrossRef](#)]
48. Goodale, C.L.; Thomas, S.A.; Fredriksen, G.; Elliott, E.M.; Flinn, K.M.; Butler, T.J.; Walter, M.T. Unusual seasonal patterns and inferred processes of nitrogen retention in forested headwaters of the Upper Susquehanna River. *Biogeochemistry* **2009**, *93*, 197–218. [[CrossRef](#)]
49. Ohte, N. Implications of seasonal variation in nitrate export from forested ecosystems: A review from the hydrological perspective of ecosystem dynamics. *Ecol. Res.* **2012**, *27*, 657–665. [[CrossRef](#)]
50. Lladó, S.; López-Mondéjar, R.; Baldrian, P. Forest Soil Bacteria: Diversity, Involvement in Ecosystem Processes, and Response to Global Change. *Microbiol. Mol. Biol. Rev.* **2017**, *81*, e00063–16. [[CrossRef](#)]

51. Richards, C.; Johnson, L.B.; Host, G.E. Landscape-scale influences on stream habitats and biota. *Can. J. Fish. Aquat. Sci.* **1996**, *53*, 295–311. [[CrossRef](#)]
52. Johnson, L.; Richards, C.; Host, G.; Arthur, J. Landscape influences on water chemistry in Midwestern stream ecosystems. *Freshw. Biol.* **1997**, *37*, 193–208. [[CrossRef](#)]
53. Craig, L.S.; Palmer, M.A.; Richardson, D.C.; Filoso, S.; Bernhardt, E.S.; Bledsoe, B.P.; Doyle, M.W.; Groffman, P.M.; Hassett, B.A.; Kaushal, S.S. Stream restoration strategies for reducing river nitrogen loads. *Front. Ecol. Environ.* **2008**, *6*, 529–538. [[CrossRef](#)]
54. Kaushal, S.S.; Groffman, P.M.; Mayer, P.M.; Striz, E.; Gold, A.J. Effects of stream restoration on denitrification in an urbanizing watershed. *Ecol. Appl.* **2008**, *18*, 789–804. [[CrossRef](#)]
55. Gergel, S.E.; Turner, M.G.; Kratz, T.K. Dissolved organic carbon as an indicator of the scale of watershed influence on lakes and rivers. *Ecol. Appl.* **1999**, *9*, 1377–1390. [[CrossRef](#)]
56. Hunsaker, C.T.; Levine, D.A. Hierarchical approaches to the study of water quality in rivers. *Bioscience* **1995**, *45*, 193–203. [[CrossRef](#)]
57. Meynendonckx, J.; Heuvelmans, G.; Muys, B.; Feyen, J. Effects of watershed and riparian zone characteristics on nutrient concentrations in the River Scheldt Basin. *Hydrol. Earth Syst. Sci.* **2006**, *10*, 913–922. [[CrossRef](#)]
58. Tong, S.T.; Chen, W. Modeling the relationship between land use and surface water quality. *J. Environ. Manag.* **2002**, *66*, 377–393. [[CrossRef](#)] [[PubMed](#)]
59. Basnyat, P.; Teeter, L.D.; Flynn, K.M.; Lockaby, B.G. Relationships between landscape characteristics and nonpoint source pollution inputs to coastal estuaries. *Environ. Manag.* **1999**, *23*, 539–549. [[CrossRef](#)]
60. Chang, M.; McCullough, J.D.; Granillo, A.B. Effects of land use and topography on some water quality variables in forested east Texas 1. *J. Am. Water Resour. Assoc.* **1983**, *19*, 191–196. [[CrossRef](#)]
61. Shih, Y.-T.; Lee, T.-Y.; Huang, J.-C.; Kao, S.-J. Apportioning riverine DIN load to export coefficients of land uses in an urbanized watershed. *Sci. Total Environ.* **2016**, *560*, 1–11. [[CrossRef](#)]
62. Hough-Snee, N.; Roper, B.; Wheaton, J.; Lokteff, R. Riparian vegetation communities of the American Pacific Northwest are tied to multi-scale environmental filters. *River Res. Appl.* **2015**, *31*, 1151–1165. [[CrossRef](#)]
63. Aschonitis, V.; Feld, C.; Castaldelli, G.; Turin, P.; Visonà, E.; Fano, E.A. Environmental stressor gradients hierarchically regulate macrozoobenthic community turnover in lotic systems of Northern Italy. *Hydrobiologia* **2016**, *765*, 131–147. [[CrossRef](#)]
64. Aber, J.D.; Nadelhoffer, K.J.; Steudler, P.; Melillo, J.M. Nitrogen saturation in northern forest ecosystems. *Bioscience* **1989**, *39*, 378–286. [[CrossRef](#)]
65. Howarth, R.W.; Sharpley, A.; Walker, D. Sources of nutrient pollution to coastal waters in the United States: Implications for achieving coastal water quality goals. *Estuaries* **2002**, *25*, 656–676. [[CrossRef](#)]
66. Huang, H.; Chen, D.; Zhang, B.; Zeng, L.; Dahlgren, R.A. Modeling and forecasting riverine dissolved inorganic nitrogen export using anthropogenic nitrogen inputs, hydroclimate, and land-use change. *J. Hydrol.* **2014**, *517*, 95–104. [[CrossRef](#)]

Publisher’s Note: MDPI stays neutral with regard to jurisdictional claims in published maps and institutional affiliations.



© 2020 by the authors. Licensee MDPI, Basel, Switzerland. This article is an open access article distributed under the terms and conditions of the Creative Commons Attribution (CC BY) license (<http://creativecommons.org/licenses/by/4.0/>).